Synthesis of Ferrosilicon from Coconut Char as Reductant at Different Reduction Times

Anis Nadhirah Ismail [a, b] *, Nik Natasya Ameera Nik Hukman Sani [a], and Mohd Hakim Ibrahim [c]

[a]Faculty of Chemical Engineering and Technology, University Malaysia Perlis (UniMAP), 02600, Arau, Perlis, Malaysia
[b]Center of Excellence Geopolymer & Green Technology (CeGeoTech), University Malaysia Perlis (UniMAP), 02600, Arau, Perlis, Malaysia
[c]Mineral Research Centre, Mineral and Geoscience Department Malaysia, Jalan Sultan Azlan Shah, 31400 Ipoh, Perak, Malaysia
∗Corresponding author. Tel.: +60-195283091; e-mail: anisnadhirah@unimap.edu.my

ABSTRACT

In the steelmaking industry, the kind of silica and carbon sources utilized in the ferrosilicon manufacturing process have a big impact on the operation's stability, energy usage, and cost. Biomass resources have gained attention due to their potential to replace existing materials to produce activated carbon as it is the best way to preserve the environment. Thus, this study focused on the synthesis of ferrosilicon from coconut char as a reductant at different reduction times (30, 60, 90 and 120 minutes). The coconut char was prepared by physical activation method via pyrolysis process at 450°C within 2 hours under a nitrogen atmosphere. X-ray Diffraction (XRD), X-ray fluorescence (XRF), and Optical Microscope (OM) were used to characterize the activated carbon from coconut shells. CHNS analysis found an increment of about 65% in carbon content after pyrolyzed, which could potentially be used as a reductant in ferrosilicon synthesis. Next, the ferrosilicon synthesis study was conducted in a muffle furnace at a reduction temperature of 1200°C with a flow rate of 10°C/min for 30, 60, 90, and 120 minutes of reduction times. Phase transformation of reduced samples at different reduction times was analyzed by X-ray Diffraction (XRD). XRD pattern found that at 120 minutes reduction times, the iron silicon peak is observed as the morphology analysis showed a presence of metallic grey particles which represent the existence of iron silicon. The possibility of converting the biomass into an alternate supply that was discovered in ferrosilicon synthesis also would minimize the landfill waste.

Keywords: *Ferrosilicon, Activated carbon, Pyrolysis, Coconut shell waste, Reductant, Different reduction times*
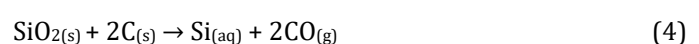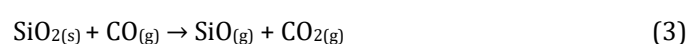
1. INTRODUCTION

The production of ferrosilicon involves a carbothermic reduction process that relies on carbon material as a reducing agent, along with silica, hematite, and charcoal as the main reactants. However, the high cost, energy consumption, and operational stability associated with the carbon content used in ferrosilicon production pose challenges [1], [2]. Previous studies have highlighted the significant energy requirements, with up to 10.5 MWh of electrical energy needed per tonne of ferrosilicon due to the endothermic nature of the reduction process [3]. Additionally, charcoal is responsible for 70% of the world's iron-carbon alloy production and contributes to 26% of industrial greenhouse gas emissions, making waste management and energy conservation crucial concerns in this sector. Ferrosilicon is widely used as an additive for silicon and as a deoxidizing element in the steel and cast-iron industries, and the reactivity of the reduction material significantly impacts the yield and cost of high silicon ferrosilicon.

Addressing the cost issues associated with ferrosilicon production, previous studies from Ratan et al., have explored the use of agricultural waste, which contains high carbon content, as an alternative reducing agent. By utilizing agricultural waste as a precursor, the cost of manufacturing activated carbon, a key component in ferrosilicon production, can be reduced. Common agricultural waste materials used include rice husks, palm shells and nut shells [4].

The production of ferrosilicon involves the reduction of iron oxide using solid carbon through direct reduction (Equation 1) and the Boudouard reaction (Equation 2). Carbon monoxide (CO) generated from the iron oxide reduction process (Equation 1) acts as an intermediary phase of silicon monoxide (SiO) and aids in the gas phase reduction of silica (SiO_2) (Equations 3 and 4). Carbon (C) facilitates the reduction of silica at high temperatures, and the reaction occurs between carbon and silica particles [5], [6]. Once SiO and CO are produced, the reaction continues at the surface of carbon and silica particles through the gas phase (Equations 2 and 3). The reduced silica then dissolves into molten iron, forming ferrosilicon [7].

$$Fe_2O_{3(s)} + 3C_{(s)} \rightarrow 2Fe(aq) + 3CO_{(g)} \tag{1}$$

$$C_{(s)} + CO_{2(g)} \rightarrow 2CO_{(g)} \tag{2}$$

$$SiO_{2(s)} + CO_{(g)} \rightarrow SiO_{(g)} + CO_{2(g)} \tag{3}$$

$$SiO_{2(s)} + 2C_{(s)} \rightarrow Si_{(aq)} + 2CO_{(g)} \tag{4}$$

Coombes et al. reported that the presence of silica promoted the iron oxide reduced to α-Fe via stable magnetite (Fe_3O_4) and wustite (FeO) phases. During the reprocessing, Fe diffuses out the amorphous silica-promoted iron oxide matrix upon reduction from Fe_{2+} and coexists with the amorphous Fe-O-Si matrix. At sufficient energy (temperature) and time the amorphous Fe-O-Si material forms iron silicate (Fe_2SiO_4) [8]. When silicon-rich conditions occurred during the process, the iron silicon ($FeSi_2$) produced [9]. Previous researchers stated that the SiO_2 mainly participates in the formation of the liquid phase that eventually affects the reduction process, depending on the reduction temperature, time and atmosphere. With high SiO_2 content, more silicate phases can be formed and melted to form molten silicate [10], [11]. Other than that, the presence of controlled silicon in molten iron can reduce the Carbon dioxide (CO_2) emissions to the atmosphere due to the decreasing of the production process led to a sustainable process [12].

In this study, the focus is on synthesizing ferrosilicon using coconut shell waste as a reductant, with different reduction times (30, 60, 90, and 120 minutes) being investigated. The pyrolysis process will be employed to produce activated carbon from coconut shells, followed by the synthesis of ferrosilicon using a muffle furnace at a temperature of 1200°C.

2. MATERIAL AND METHODS

2.1. Preparing Coconut Char via Pyrolysis Process

Coconut shell wastes used as reductants in the ferrosilicon synthesis were collected from Perlis, Malaysia. The coconut shell was dried in an oven for 24 hours and crushed into approximately 2 mm particle size, as shown in Figure 1 (a). The coconut shell waste was converted into coconut char via the pyrolysis process by using a horizontal tube furnace with an injection of nitrogen (N_2) gas (flow rate of 0.1 L/min) at a temperature of 450°C for 2 hours soaking time. Figure 1 (b) shows the coconut char samples after the pyrolysis process.

2.2. Sample Preparations and Characterizations

The materials used for the synthesis of ferrosilicon were coconut char as carbon source, hematite (Fe_2O_3 - 85.9%) as
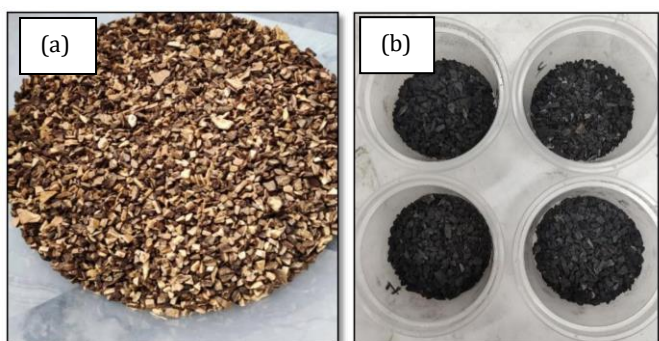

Figure 1. (a) Raw coconut shell before the pyrolysis and (b) coconut char after the pyrolysis

iron oxide source and silica powder (99.8%) as silica source. All raw materials were ground into a powder and sieved to get fine particles of less than 63μm. Next, using the mass ratio of (6.5C: $1.8Fe_2O_3$: $2.9SiO_2$), the coconut char, hematite, and silica were added into a planetary ball mill machine. To achieve uniform and homogeneous mixing, the ball mill's speed was adjusted to 250 rpm for one hour.

Table 1 and Table 2 exhibit the results of the ultimate and chemical analysis of coconut shell and coconut char performed with the CHNS elemental analyzer and XRF respectively. After pyrolyzing, the CHNS analysis revealed a roughly 65% increase in carbon content.

2.3. Ferrosilicon Synthesis

For the synthesis of the ferrosilicon study, a muffle furnace was employed. At four distinct reduction times (30, 60, 90, 120 min), the sample was put in a ceramic crucible and driven into the furnace at a temperature of 1200°C for reduction. The reduced samples were analysed by X-ray diffractometer and Optical Microscope. The percentage of reduction was also determined.

3. RESULTS AND DISCUSSION

3.1. Phase Transformation

The XRD pattern of the reduced samples at 1200°C. Fe_3O_4 and SiO_2 were the main reactions in ferrosilicon synthesis. The phase transformation of samples at different reduction times (30, 60, 90 and 120 minutes) is presented in Figure 2 while Table 3 presents the list of peak positions available in the reaction product.

From Figure 2, as for the 30 and 60 minutes reduction times, SiO_2 and Fe_2O_3 are the main reaction products for both reduction times showing that the reaction was not fully

Table 1. Ultimate analysis of coconut shell and coconut char

Materials	Coconut shell	Coconut char
Carbon (wt.%)	47.4	78.6
Hydrogen (wt.%)	0.1	2.1
Hydrogen (wt.%)	0.5	0.1
Sulphur (wt.%)	6.4	1.5

Table 2. Chemical composition of coconut shell

Chemical compound	wt.%
K_2O	24.29
SiO_2	19.68
MgO	14.22
Al_2O_3	3.03
Fe_2O_3	3.00
CaO	2.45
SO_3	1.61
P_2O_5	0.86

reduced due to insufficient reduction time. However, after 90 minutes of reduction times, Fe_2SiO_4 phase was identified. A linear and sharp peak of Fe_2SiO_4 appeared ($2\theta = 36.26°$ and $54.01°$) in the reduced sample due to the reduction of Fe_2O_3 and initial SiO_2 reduction with the disappearance of a few Fe_2O_3 and SiO_2 peaks. The synthesis of Fe_2SiO_4 phase occurred from the cooperation of silica and iron oxide crystallites thus exhibits the iron-silica interaction during the reduction process [8], [13]. Previous research states that when iron and silicon are formed due to inter-diffusion during solidification, several iron silicates such as Fe_2SiO_4 can be formed [5]. Additionally, this transformation occurs only when energy (temperature) and reduction time are sufficient.

As the reduction time extended into 120 minutes, the $FeSi_2$ phase was identified at angles $22.02°$, $28.5°$, $31.49°$, $36.45°$, $49.41°$ and $54°$ with the disappearance of Fe_2O_3 and Fe_2SiO_4 peaks (Figure 2 and Table 3). Increasing reduction time resulted in more hematite and silica reduction and the formation of Fe_2SiO_4 phase, which subsequently transformed into $FeSi_2$. This indicates that with longer reduction times, the silicon-rich condition occurred, leading to the formation of $FeSi_2$ [9], [14]. The presence of the FeSi2 phase was evident in the reaction product at a reduction time of 120 minutes.

3.2. Microstructure Analysis

Figure 3 shows the micrograph of the reduced samples at different reduction times (30, 60, 90 and 120 minutes) by using hematite as the iron oxide source, silica powder as the silica source, and coconut char as the carbon reductant, which was taken at 2x magnification. The finding revealed the main colours observed in the reduced samples.

The samples at 30 (Figure 3 (a)) and 60 (Figure 3 (b)) minutes of reduction time exhibited white, black, and red colours. The white colour indicated the presence of silica (SiO_2), while black and red represented carbon (C) and hematite (Fe_2O_3) elements, respectively. There was no significant difference observed between the reduced samples at reduction times of 30 and 60 minutes due to the shorter reduction time. As the reduction time increased to 90 minutes, a dark grey colour corresponding to the iron silicate (Fe_2SiO_4) element was observed in the reduced sample (Figure 3 (c)). The presence of silica resulted in the formation of Fe_2SiO_4 [15]. Additionally, the micrograph for the 120 minutes reduction time displayed a metallic grey colour, indicating the existence of iron silicon ($FeSi_2$) (Figure 3 (d)). These findings were consistent with the X-ray Diffraction (XRD) data, which showed the presence of the iron silicate (Fe_2SiO_4) and iron silicon ($FeSi_2$) phases in
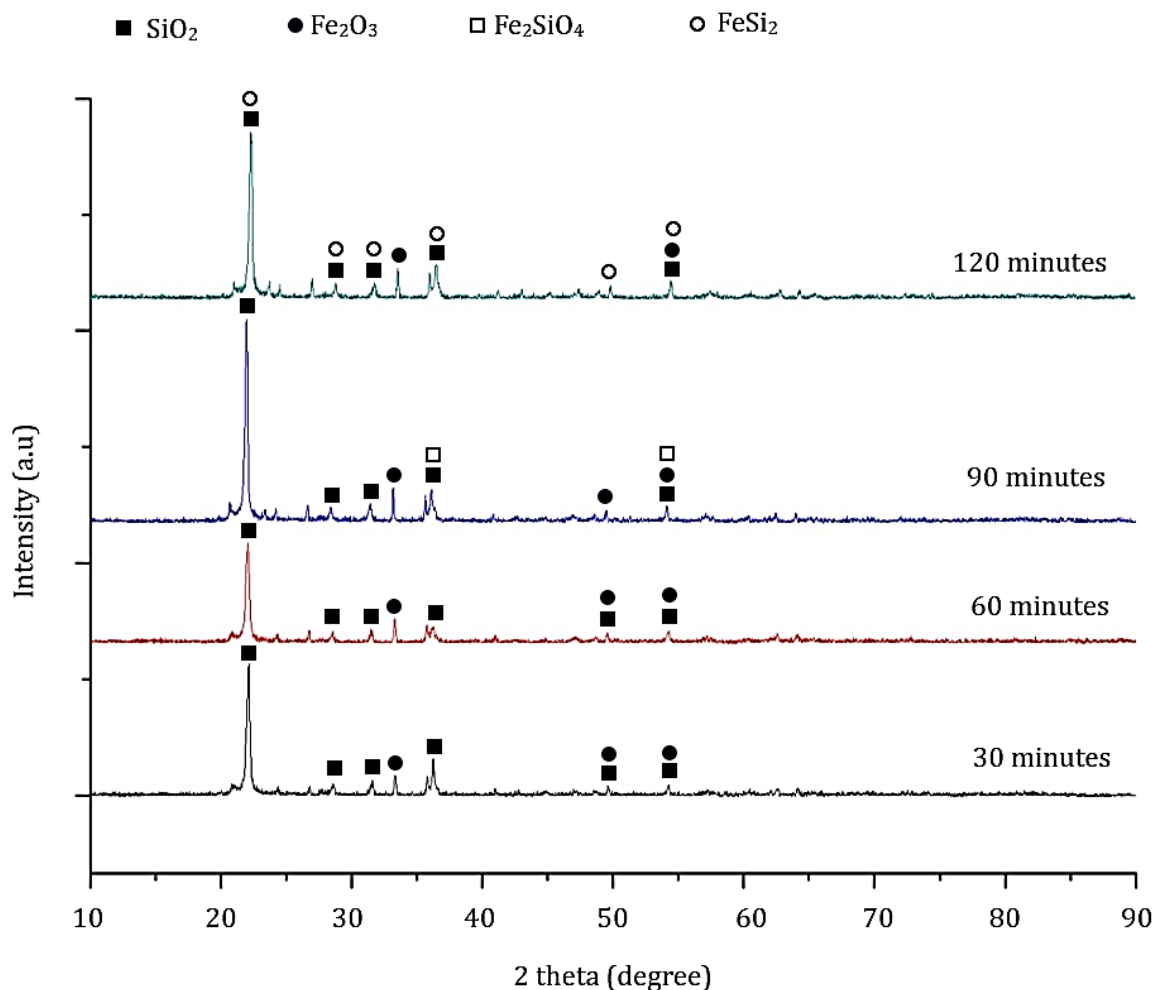

Figure 2. X-ray diffraction of reduced sample at 30, 60, 90 and 120 min of reduction times

Table 3. Peak position available in reduced samples at different reduction times (30, 60, 90 and 120 minutes)

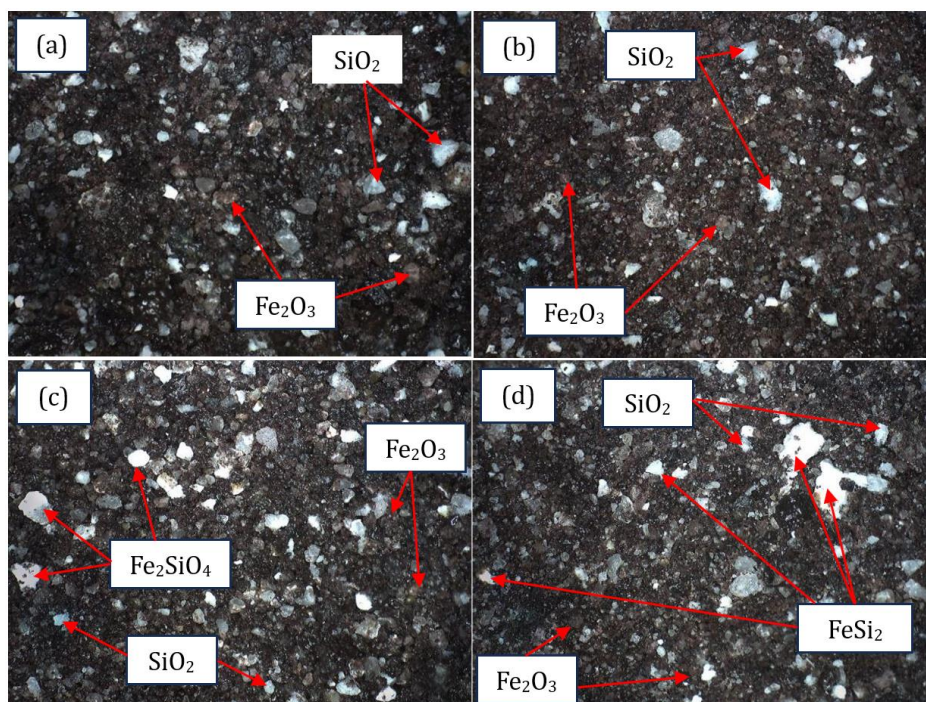| Chemical Compound	30 min		60 min		90 min		120 min	
	Angle (2θ)	Plane (hkl)	Angle (2θ)	Plane (hkl)	Angle (2θ)	Plane (hkl)	Angle (2θ)	Plane (hkl)
SiO_2	22°	1 0 1	22.02°	1 0 1	21.90°	1 0 1	22.02°	1 0 1
	28.24°	1 1 1	28.49°	1 1 1	28.34°	1 1 1	28.5°	1 1 1
	31.5°	1 0 5	31.49°	1 0 2	31.5°	1 0 2	31.49°	1 0 2
	36°	2 0 0	36.16°	2 0 0	36.26°	2 0 0	36.45°	2 0 0
	49.44°	1 1 2	49.41°	1 1 2	54.01°	2 0 3	54°	2 0 3
	54.2°	2 0 2	54.05°	2 0 2				
Fe_2O_3	33.14°	1 0 4	33.12°	1 0 4	33.12°	1 0 4	33.12°	1 0 4
	49.44°	0 2 4	49.41°	0 2 4	49.4°	0 2 4	54°	1 1 6
	54.2°	1 1 6	54.05°	1 1 6	54.01°	1 1 6		
Fe_2SiO_4	-	-	-	-	36.26°	3 1 1	-	-
					54.01°	4 2 2		
$FeSi_2$	-	-	-	-	-	-	22.02°	0 0 2
							28.5°	2 0 2
							31.49°	3 1 1
							36.45°	4 0 0
							49.41°	2 1 2
							54°	5 1 2

Figure 3. Microstructure of reduced sample at (a) 30 min, (b) 60 min, (c) 90 min and (d) 120 min of reduction times

the reduced samples synthesized at 1200°C for 90 and 120 minutes, respectively. These results suggest that iron and silicon reduction begins after one hour of synthesis time and thus exhibits iron-silica interaction to form the iron silicate and iron silicon.

3.3. Percentage of Reduction (%)

The graph presented in Figure 4 illustrates the percentage of reduction for the reduced sample at four different reduction times (30, 60, 90 and 120 minutes) at a reduction temperature of 1200°C. The sample weight loss of the samples was used to compute the percentage of reduction as formulated in Equation 5. To calculate the weight loss, the samples' reduced weights before and after were recorded.

$$\text{Percentage of Reduction (\%)} = [W – W_o]/W * 100 \qquad (5)$$

where;
W = weight of the sample before reduction (g)
W_o = weight of sample after reduction (g)

From Figure 4, the data show a gradual increase in the reduction percentage pattern as the reduction time increases. The percentage of reduction for the samples subjected to 30, 60, 90 and 120 minutes of reduction time are 90%, 92%, 93% and 95% respectively. The longer residence times allow for more contact between the hematite, silica and the reducing agent, promoting more reduction of hematite and silica thus resulting higher percentage of reduction. The presence of higher carbon
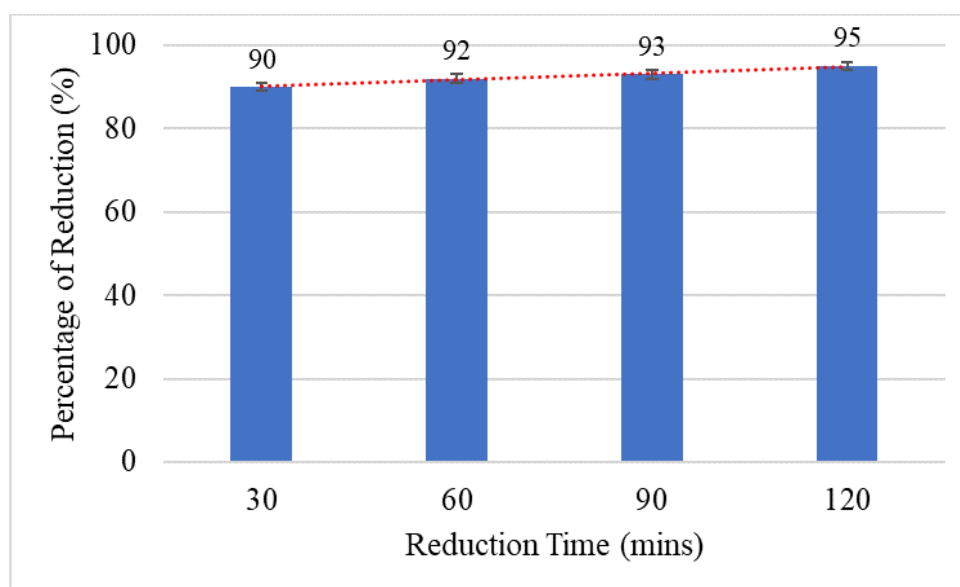
Figure 4. Reduction percentage (%) for the reduced samples at different reduction times (30, 60, 90 and 120 minutes)

content, particularly from the coconut char used in this study, contributes to mass loss through the elimination of moisture and volatile matter during devolatilization. The porous structure of the coconut char facilitates fast diffusion and efficient reduction of iron oxide through the reducing gases. The results align with previous research, indicating that higher carbon content leads to greater reduction percentages and longer reduction times result in increased reduction percentages [16], [17]. These findings are consistent with the X-ray Diffraction (XRD) analysis, where phase transformations occur due to the release of carbon monoxide (CO) and other gases during the reduction process. The generation of more ferrosilicon is observed with higher amounts of gases, accompanied by a decrease in sample weight.

4. CONCLUSION

The synthesis ferrosilicon phases can be developed during the reduction reaction at a temperature of 1200°C within 90 - 120 minutes reaction time using coconut char as carbon materials, silica powder as the silica source, and hematite as the iron oxide source. XRD analysis confirmed the development of iron silicate (Fe_2SiO_4) and iron silicon ($FeSi_2$) phases during ferrosilicon synthesis at 90 and 120 minutes of reduction times, respectively. The dark grey colour and metallic grey colour were observed as Fe_2SiO_4 and $FeSi_2$ phases in the micrograph of 90 and 120 minutes reduction times reaction product respectively. The reduction time of 120 minutes showed the highest reduction percentage due to more weight loss during the reduction process compared to others. In conclusion, the duration of the reduction process played a crucial role, in influencing the reaction extent and the reaction product. Increasing the reduction time from 30 to 120 minutes resulted in enhanced reaction progress and yielding the ferrosilicon. On the other hand, ferrosilicon synthesis may benefit from the use of carbon material derived from agricultural waste. Therefore, it is preferable to use the alternate carbon source in a sustainable ferrosilicon production method.

REFERENCES

[1] G. R. Surup, A. Trubetskaya, and M. Tangstad, "Charcoal as an Alternative Reductant in Ferroalloy Production: A Review," *Processes*, vol. 8, no. 11, p. 1432, Nov. 2020.

[2] M. Tangstad, J. P. Beukes, J. Steenkamp, and E. Ringdalen, "14 - Coal-based reducing agents in ferroalloys and silicon production," I. Suárez-Ruiz, M. A. Diez, and F. B. T.-N. T. in C. C. Rubiera, Eds., Woodhead Publishing, 2019, pp. 405–438.

[3] K. He and L. Wang, "A review of energy use and energy-efficient technologies for the iron and steel industry," *Renewable and Sustainable Energy Reviews*, vol. 70, pp. 1022–1039, 2017.

[4] J. K. Ratan, M. Kaur, and B. Adiraju, "Synthesis of activated carbon from agricultural waste using a simple method: Characterization, parametric and isotherms study," *Materials Today: Proceedings*, vol. 5, no. 2, Part 1, pp. 3334–3345, 2018.

[5] N. F. M. Yunos, M. A. Idris, S. R. R. Munusamy, and K. Perumal, "Effect of using Palm Char and Coke as a Reductant in Production of Ferrosilicon," *IOP Conference Series: Materials Science and Engineering*, vol. 957, no. 1, p. 12031, 2020.

[6] R. Farzana, R. Rajarao, and V. Sahajwalla, "Characteristics of waste automotive glasses as silica resource in ferrosilicon synthesis," *Waste Management & Research*, vol. 34, no. 2, pp. 113–121.

[7] A. N. Ismail, M. H. Ibrahim, R. Mohd Said, F. Somidin, and S. A. Ismail, "Influence of recycled wastes on ferrosilicon production in steel making applications: A short review," *Journal of Physics: Conference Series*, vol. 2169, no. 1, p. 12028, 2022.

[8] M. J. Coombes, E. J. Olivier, E. Prestat, S. J. Haigh, E. du Plessis, and J. H. Neethling, "Iron-silica interaction during reduction of precipitated silica-promoted iron oxides using in situ XRD and TEM," *Applied Catalysis A: General*, vol. 613, p. 118031, 2021.

[9] N. Dahal and V. Chikan, "Phase-Controlled Synthesis of Iron Silicide (Fe3Si and FeSi2) Nanoparticles in Solution," *Chemistry of Materials*, vol. 22, no. 9, pp. 2892–2897, May 2010.

[10] H. Long, X. Wu, T. Chun, Z. Di, and B. Yu, "Assimilation Behavior of Calcium Ferrite and Calcium Diferrite with Sintered Al2O3 and MgO," *Metallurgical and Materials Transactions B*, vol. 47, no. 5, pp. 2830–2836, 2016.

[11] B. Yu, X. Lv, S. Xiang, C. Bai, and J. Yin, "Wetting Behavior of Calcium Ferrite Melts on Sintered MgO," *ISIJ International*, vol. 55, no. 8, pp. 1558–1564, 2015.

[12] A. P. M. Diniz, K. F. Côco, F. S. V. Gomes, and J. L. F. Salles, "Forecasting Model of Silicon Content in Molten Iron Using Wavelet Decomposition and Artificial Neural Networks," *Metals*, vol. 11, no. 7, p. 1001, Jun. 2021.

[13] H. Dlamini, T. Motjope, G. Joorst, G. ter Stege, and M. Mdleleni, "Changes in Physico-Chemical Properties of Iron-Based Fischer–Tropsch Catalyst Induced by SiO2 Addition," *Catalysis Letters*, vol. 78, no. 1, pp. 201–207, 2002.

[14] J. Liu *et al.*, "Effect of Silica Content on Iron Ore Sintering," *Metals*, vol. 13, no. 6, p. 1009, May 2023.

[15] C.-H. Zhang, H.-J. Wan, Y. Yang, H.-W. Xiang, and Y.-W. Li, "Study on the iron–silica interaction of a co-precipitated Fe/SiO2 Fischer–Tropsch synthesis catalyst," *Catalysis Communications*, vol. 7, no. 9, pp. 733–738, 2006.

[16] N. H. Najmi, N. F. D. Mohd Yunos, N. K. Othman, A. Ismail, and A. Idris, "Agricultural waste as iron reductant for producing metallic iron in steelmaking," *Journal of Engineering and Applied Sciences*, vol. 11, pp. 9770–9775, Aug. 2016.

[17] D. Fu *et al.*, "Diffusion and phase transformations during the reaction between ferrosilicon and CaO·MgO under vacuum," *Journal of Materials Research and Technology*, vol. 9, no. 3, pp. 4379–4385, 2020.